

GENERALIZED LINDLEY-POISSON DISTRIBUTION  
AND ITS APPLICATIONS

M. E. Ghitany <sup>1,§</sup>, A. Asgharzadeh <sup>2</sup>, A. Saadati Nik <sup>2</sup>

<sup>1</sup> Department of Statistics and Operations Research

Faculty of Science, Kuwait University, KUWAIT

e-mail: [me.ghitany@ku.edu.kw](mailto:me.ghitany@ku.edu.kw)

<sup>2</sup> Department of Statistics

University of Mazandaran, Babolsar, IRAN

**Abstract**

In this paper, we consider a survival model of competing risks where the number of causes of failure is random,  $M$ , and only the minimum of the survival times due to various causes,  $Y = \min(X_1, X_2, \dots, X_M)$ , is observed. Considering the distribution of  $M$  as zero-truncated Poisson and the baseline distribution of  $X$  as generalized Lindley, a generalized Lindley-Poisson distribution is obtained. The structural properties of the proposed model are studied. The method of maximum likelihood is used to estimate the parameters of the proposed model. Simulation studies are carried out to study the performance of the estimators. Two real data sets are analyzed and it is shown that the proposed model fits better than some of the existing models.

**MSC 2020:** 62F10, 62E20

**Key Words and Phrases:** generalized Lindley distribution; zero-truncated Poisson distribution; compounding; maximum likelihood

## 1. Introduction

In survival analysis, the complete survival times  $X_1, X_2, \dots, X_M$  are usually not available. However,  $Y = \min(X_1, X_2, \dots, X_M)$  is observed. This situation arises in competing risk theory where  $X_1, X_2, \dots, X_M$  are the survival times due to different causes of failure and only  $Y$  is observed along with the cause of failure. The number of observations is unknown and so  $M$  is considered as a discrete random variable with support  $\{1, 2, \dots\}$ .

In this paper, we consider a random sample where only  $X$  is observed and  $M$  is considered as random. More specifically, let  $X_1, X_2, \dots, X_M$  be a random sample of size  $M$  from a base distribution with survival function (s.f.)  $S_X(x)$ . Then, the conditional survival function of  $Y$  is given by

$$S_{Y|M}(y|m) = [S_X(y)]^m.$$

The unconditional survival function of  $Y$  is given by

$$\begin{aligned} S_Y(y) &= \sum_{m=1}^{\infty} [S_X(y)]^m P(M = m) \\ &= G_M(S_X(y)), \end{aligned} \quad (1)$$

where  $G_M(s) = \sum_{m=1}^{\infty} s^m P(M = m)$ ,  $0 < s < 1$ , is the probability generating function (p.g.f.) of  $M$ .

The model above with s.f. (1) can be interpreted as a proportional hazard model whose hazard rate is given by

$$h_{Y|M}(y|M) = M h_X(y),$$

where  $h_X(x) = -\frac{d}{dx} \log S_X(x)$  is the baseline hazard rate function (h.r.f.) and  $M$  is the proportionality factor, whence in this case is random and has a discrete distribution. This is analogous to the proportional hazard continuous frailty model, see [11].

Various distributions of  $X$  and  $M$  have been considered in the literature. For example, [2], [16], [20], [6], [8], and [5] have considered the baseline distribution of  $X$  as exponential and the distribution of  $M$  as geometric, Poisson, logarithmic, power series, Conway-Maxwell-Poisson, and Poisson-Lindley, respectively. Also, [18], [12] [13], [14], and [3] have considered the baseline distribution of  $X$  as Weibull and the distribution of  $M$  as power series, generalized Poisson, Conway-Maxwell-Poisson, Bessel, and generalized Sibuya, respectively. In addition, [10] and [21] have considered the baseline distribution of  $X$  as Lindley and the distribution of  $M$  as Poisson and power series, respectively. The paper [19] has considered the baseline distribution of  $X$  as exponentiated power Lindley and the distribution of  $M$  as Poisson.

In the present paper, we consider a model with baseline distribution as two-parameter generalized Lindley and the distribution of  $M$  as (zero-truncated)

Poisson giving rise to a three parameter model. The hazard rate function of this model has monotone and non-monotone shapes.

The contents of this paper are organized as follows. Section 2 contains the development of the generalized Lindley-Poisson distribution and its structural properties. Maximum likelihood estimation of the model's parameters is presented in Section 3. Simulation studies are carried out in Section 4 to examine the performance of the estimators. Two real data applications are presented in Section 5. Finally, some conclusions and comments are provided in Section 6.

## 2. The model and its properties

Let the random variable  $M$  follows zero-truncated Poisson distribution with probability mass function (p.m.f.)

$$P(M = m) = \frac{\theta^m}{m!(e^\theta - 1)}, \quad m = 1, 2, 3, \dots, \quad \theta > 0,$$

and p.g.f.

$$G_M(s) = \frac{e^{\theta s} - 1}{e^\theta - 1}, \quad 0 < s < 1, \quad \theta > 0. \quad (2)$$

The baseline distribution of  $X$  is assumed to have a two-parameter generalized Lindley distribution with p.d.f.

$$f_X(x) = \frac{\lambda^2}{\lambda + \alpha} (1 + \alpha y) e^{-\lambda y}, \quad x > 0, \quad \alpha, \lambda > 0,$$

and s.f.

$$S_X(x) = \left(1 + \frac{\alpha \lambda}{\lambda + \alpha} y\right) e^{-\lambda y}, \quad x > 0, \quad \alpha, \lambda > 0. \quad (3)$$

Using (1), (2), (3), the s.f. of  $Y$  is given by

$$\begin{aligned} S_Y(y) &= G_M(S_X(y)) \\ &= \frac{e^{\theta(1 + \frac{\alpha \lambda}{\lambda + \alpha} y) e^{-\lambda y}} - 1}{e^\theta - 1}, \quad y > 0, \quad \alpha, \lambda, \theta > 0. \end{aligned}$$

**2.1. Probability density function.** For all  $y, \alpha, \lambda, \theta > 0$ , the p.d.f. of  $Y$  is given by

$$\begin{aligned} f_Y(y) &= -S'_Y(y) \\ &= \frac{\theta \lambda^2}{(e^\theta - 1)(\lambda + \alpha)} (1 + \alpha y) e^{-\lambda y} e^{\theta(1 + \frac{\alpha \lambda}{\lambda + \alpha} y) e^{-\lambda y}}. \end{aligned} \quad (4)$$

The distribution with p.d.f. (4) will be called generalized Lindley-Poisson, denoted by  $GLP(\alpha, \lambda, \theta)$ . Note that when  $\alpha = 1$ , we obtain the Lindley-Poisson distribution introduced by [10].

The following theorem gives sufficient conditions for all possible shapes of the p.d.f. of the GLP distribution.

**THEOREM 2.1.**  $f_Y(y)$  is decreasing (unimodal) if  $\lambda^2(1 + \theta) \geq \alpha^2$  ( $\lambda^2(1 + \theta) < \alpha^2$ ) with

$$f_Y(0) = \frac{\theta e^\theta \lambda^2}{(e^\theta - 1)(\lambda + \alpha)}, \quad f_Y(\infty) = 0.$$

**P r o o f.** Let

$$\xi(y) = \log f_Y(y) = \text{Const} + \log(1 + \alpha y) - \lambda y + \theta \left(1 + \frac{\alpha \lambda}{\lambda + \alpha} y\right) e^{-\lambda y}.$$

The first derivative of  $\xi(y)$  is

$$\xi'(y) = \frac{d \log f_Y(y)}{dy} = \frac{e^{-\lambda y} g(y)}{(\lambda + \alpha)(1 + \alpha y)},$$

where

$$g(y) = e^{\lambda y}(\alpha + \lambda)[\alpha - \lambda(\alpha y + 1)] - \theta \lambda^2(\alpha y + 1)^2.$$

Clearly, the sign of  $\xi'(y)$  is that of  $g(y)$ . The function  $g(y)$  is decreasing, since

$$g'(y) = -\alpha \lambda [e^{\lambda y}(\alpha + \lambda) + 2\theta \lambda(\alpha y + 1)] < 0.$$

Since  $g(0) = \alpha^2 - \lambda^2(1 + \theta)$  and  $g(\infty) = -\infty$ , it follow that  $g(y)$  is negative (changes sign from positive to negative) if  $g(0) \leq 0$  (if  $g(0) > 0$ ). That is, if  $\lambda^2(1 + \theta) \geq \alpha^2$  ( $\lambda^2(1 + \theta) < \alpha^2$ ).  $\square$

Figure 1 shows the p.d.f. of GLP distribution for selected values of the parameters  $\alpha$ ,  $\lambda$ ,  $\theta$ .

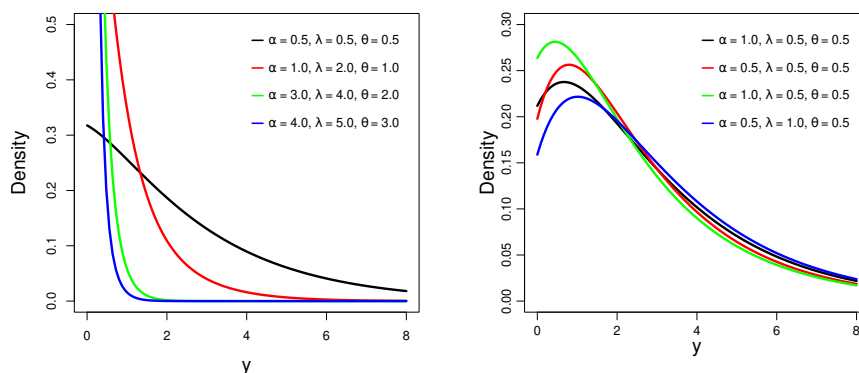


FIGURE 1. Probability density function of GLP distribution.

**2.2. Hazard rate function.** For all  $\alpha, \lambda, \theta > 0$ , the h.r.f. of  $Y$  is given by

$$\begin{aligned} h_Y(y) &= f_Y(y)/S_Y(y) \\ &= \frac{\theta \lambda^2}{\lambda + \alpha} \frac{(1 + \alpha y) e^{-\lambda y} e^{\theta \left(1 + \frac{\alpha \lambda}{\lambda + \alpha} y\right) e^{-\lambda y}}}{e^{\theta \left(1 + \frac{\alpha \lambda}{\lambda + \alpha} y\right) e^{-\lambda y}} - 1}, \end{aligned}$$

with

$$h_Y(0) = \frac{\theta e^{\theta} \alpha \lambda^2}{(e^{\theta} - 1)(\lambda + \alpha)}, \quad h_Y(\infty) = \lambda.$$

Figure 2 shows the h.r.f. of GLP distribution for selected values of  $\alpha$ ,  $\lambda$  and  $\theta$ . This figure shows that the h.r.f. can be decreasing, increasing, decreasing-increasing (bathtub), or increasing-decreasing-increasing shape.

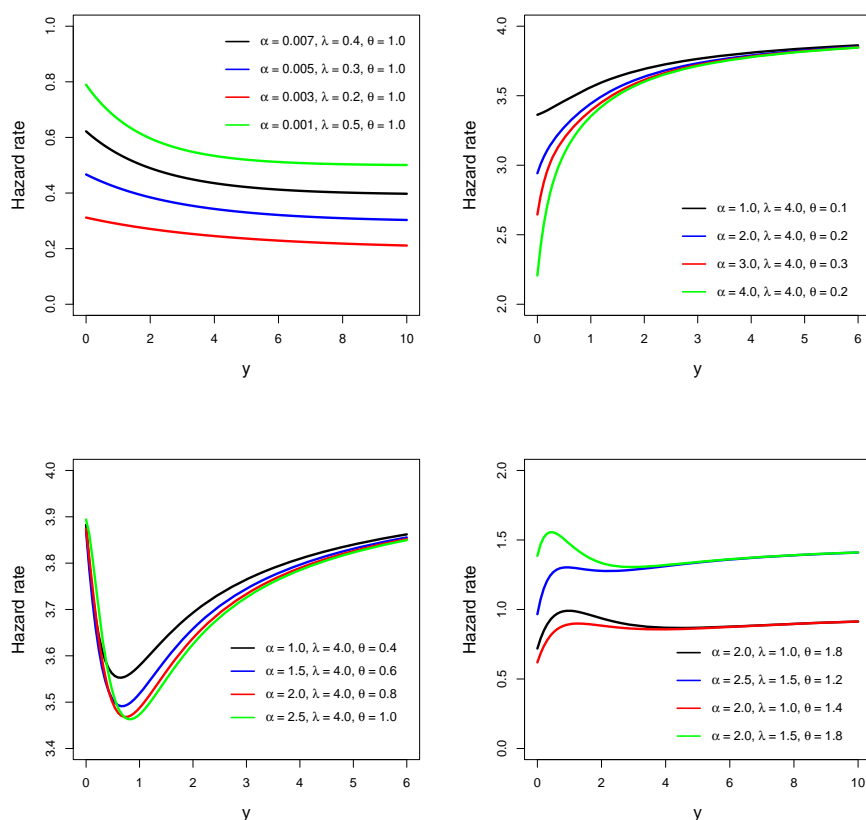


FIGURE 2. Hazard rate function of GLP distribution.

**2.3. Quantile function.** The following theorem gives explicit expression for the quantile function of the GLP distribution.

**THEOREM 2.2.** *For any  $\alpha, \lambda, \theta > 0$  and  $0 < q < 1$ , the quantile function of  $GLP(\alpha, \lambda, \theta)$  distribution is given by*

$$Q_Y(q) = \frac{1}{\alpha\lambda} \left[ -\alpha - \lambda - \alpha W_{-1} \left( -\frac{1 + \lambda/\alpha}{e^{1+\lambda/\alpha}} \cdot \frac{\log(e^\theta(1-q) + q)}{\theta} \right) \right],$$

where  $W_{-1}(\cdot)$  denotes the negative branch of the Lambert  $W$  function.

**P r o o f.** The quantile function is the solution in  $y_q$  of the equation  $1 - S_Y(y_q) = q$  for  $0 < q < 1$ . That is, the solution of

$$(1 + \lambda/\alpha + \lambda y_q) e^{-\lambda y_q} = (1 + \lambda/\alpha) \frac{\log(e^\theta(1-q) + q)}{\theta}.$$

After multiplying both sides of this equation by  $-e^{-(1+\lambda/\alpha)}$ , we obtain  $W(z) e^{W(z)} = z$ , where

$$W(z) = -(1 + \lambda/\alpha + \lambda y_q), \quad z = -\frac{1 + \lambda/\alpha}{e^{1+\lambda/\alpha}} \cdot \frac{\log(e^\theta(1-q) + q)}{\theta}.$$

Since,  $1 + \lambda/\alpha + \lambda y_q > 1$  and  $z \in [-\frac{1}{e}, 0)$ , it follows that

$$W_{-1}(z) = -(1 + \lambda/\alpha + \lambda y_q).$$

That is  $y_q = \frac{1}{\alpha\lambda} [-\alpha - \lambda - \alpha W_{-1}(z)]$ . □

**Remarks:**

- (1) Since  $-\frac{1}{e} \leq z < 0$ , it follows that  $W_{-1}(z)$  is unique, see [7], which implies that  $Q_Y(q)$  is also unique.
- (2) The median of GLP distribution is given by  $Q_Y(0.5)$
- (3) For  $\alpha = 1$ ,

$$Q_Y(q) = \frac{1}{\lambda} \left[ -1 - \lambda - W_{-1} \left( -\frac{1 + \lambda}{e^{1+\lambda}} \cdot \frac{\log(e^\theta(1-q) + q)}{\theta} \right) \right],$$

which is the quantile function of Lindley-Poisson distribution, see [10].

**2.4. Moments and associated measures.** If  $Y \sim GLP(\alpha, \lambda, \theta)$ , then the  $r$ th moment of  $Y$  is given by

$$\begin{aligned}\mu'_r = E(Y^r) &= r \int_0^\infty y^{r-1} S_Y(y) dy \\ &= \frac{r}{e^\theta - 1} \int_0^\infty y^{r-1} \left[ e^{\theta \left(1 + \frac{\alpha\lambda}{\lambda + \alpha}\right) y} e^{-\lambda y} - 1 \right] dy \\ &= \frac{r}{e^\theta - 1} \sum_{j=1}^\infty \sum_{k=0}^j c_{jk}(\alpha, \lambda, \theta) \int_0^\infty y^{k+r-1} e^{-j\lambda y} dy \\ &= \frac{r}{e^\theta - 1} \sum_{j=1}^\infty \sum_{k=0}^j c_{jk}(\alpha, \lambda, \theta) \frac{(k+r-1)!}{(j\lambda)^{k+r}},\end{aligned}$$

where the coefficients  $c_{jk}(\alpha, \lambda, \theta)$  are given by

$$c_{jk}(\alpha, \lambda, \theta) = \frac{\theta^j}{k! (j-k)!} \left( \frac{\alpha\lambda}{\lambda + \alpha} \right)^k, \quad 0 \leq k \leq j. \quad (5)$$

The mean, variance, skewness and kurtosis measures are:

$$\begin{aligned}\text{Mean} &= \mu'_1, \\ \text{Variance} &= \mu'_2 - \mu^2, \\ \text{Skewness} &= \frac{\mu'_3 - 3\mu'_2 \mu + 2\mu^3}{\sigma^3}, \\ \text{Kurtosis} &= \frac{\mu'_4 - 4\mu\mu'_3 + 6\mu^2\mu'_2 - 3\mu^4}{\sigma^4}.\end{aligned}$$

TABLE 1. Mean, variance, skewness and kurtosis of GLP distribution for selected values of the parameters.

$\alpha$	$\lambda$	$\theta$	Mean	Variance	Skewness	Kurtosis
0.5	0.5	0.5	2.665	6.223	1.789	7.656
	1		1.178	1.372	1.940	8.480
	10		0.092	0.010	2.189	10.188
1	0.5	1	2.652	5.934	1.840	8.032
	1		1.177	1.355	1.978	8.755
	10		0.084	0.009	2.390	11.591
2	0.5	5	1.245	1.477	2.887	19.390
	1		0.531	0.332	3.173	22.218
	10		0.031	0.002	4.505	40.829

### 3. Maximum likelihood estimation

Let  $y_1, y_2, \dots, y_n$  be a random sample of size  $n$  from GLP distribution with parameters  $\omega \equiv (\alpha, \lambda, \theta)$ . The log-likelihood function is given by

$$\begin{aligned}\ell_n(\phi) &= \sum_{i=1}^n \log f_Y(y_i; \phi) \\ &= n[\log(\theta) - \log(e^\theta - 1) + 2\log(\lambda) - \log(\lambda + \alpha)] \\ &\quad + \sum_{i=1}^n \log(1 + \alpha y_i) - \lambda \sum_{i=1}^n y_i + \theta \sum_{i=1}^n \left(1 + \frac{\alpha \lambda y_i}{\lambda + \alpha}\right) e^{-\lambda y_i}.\end{aligned}$$

The score vector

$$U_n(\phi) = \left( \frac{\partial \ell_n(\phi)}{\partial \alpha}, \frac{\partial \ell_n(\phi)}{\partial \lambda}, \frac{\partial \ell_n(\phi)}{\partial \theta} \right)^\top,$$

has elements

$$\frac{\partial \ell_n(\phi)}{\partial \alpha} = -\frac{n}{\lambda + \alpha} + \sum_{i=1}^n \frac{y_i}{1 + \alpha y_i} + \frac{\theta \lambda^2}{(\lambda + \alpha)^2} \sum_{i=1}^n y_i e^{-\lambda y_i},$$

$$\frac{\partial \ell_n(\phi)}{\partial \lambda} = \frac{n(\lambda + 2\alpha)}{\lambda(\lambda + \alpha)} - \sum_{i=1}^n y_i - \frac{\theta \lambda}{\lambda + \alpha} \sum_{i=1}^n \left( \frac{\lambda + 2\alpha}{\lambda + \alpha} + \alpha y_i \right) y_i e^{-\lambda y_i},$$

$$\frac{\partial \ell_n(\phi)}{\partial \theta} = n \left( \frac{1}{\theta} - \frac{e^\theta}{e^\theta - 1} \right) + \sum_{i=1}^n \left( 1 + \frac{\alpha \lambda y_i}{\lambda + \alpha} \right) e^{-\lambda y_i}.$$

The maximum likelihood estimate (MLE)  $\hat{\phi}$  of  $\omega$  can be obtained by solving the system of equations  $U_n(\phi) = 0$  numerically.

Elements of the Hessian matrix are given by



$$\begin{aligned}
\frac{\partial^2 \ell_n(\phi)}{\partial \alpha^2} &= \frac{n}{(\lambda + \alpha)^2} - \sum_{i=1}^n \frac{y_i^2}{(1 + \alpha y_i)^2} - \frac{2\theta \lambda^2}{(\lambda + \alpha)^3} \sum_{i=1}^n y_i e^{-\lambda y_i}, \\
\frac{\partial^2 \ell_n(\phi)}{\partial \lambda^2} &= -\frac{n(2\alpha^2 + 4\alpha\lambda + \lambda^2)}{\lambda(\lambda + \alpha)^2} - \frac{2\alpha^2 \theta}{(\lambda + \alpha)^3} \sum_{i=1}^n y_i e^{-\lambda y_i} \\
&\quad + \frac{\theta(-\alpha^3 + \alpha^2 \lambda + 3\alpha \lambda^2 + \lambda^3)}{(\lambda + \alpha)^3} \sum_{i=1}^n y_i^2 e^{-\lambda y_i} \\
&\quad + \frac{\theta \lambda(\alpha^3 + 2\alpha^2 \lambda + \alpha \lambda^2)}{(\lambda + \alpha)^3} \sum_{i=1}^n y_i^3 e^{-\lambda y_i}, \\
\frac{\partial^2 \ell_n(\phi)}{\partial \theta^2} &= n \left( -\frac{1}{\theta^2} + \frac{e^\theta}{(e^\theta - 1)^2} \right), \\
\frac{\partial^2 \ell_n(\phi)}{\partial \alpha \partial \lambda} &= \frac{n}{(\lambda + \alpha)^2} + \frac{\theta \lambda}{(\lambda + \alpha)^3} \sum_{i=1}^n (2\alpha - \lambda(\lambda + \alpha)y_i) y_i e^{-\lambda y_i}, \\
\frac{\partial^2 \ell_n(\phi)}{\partial \alpha \partial \theta} &= \frac{\lambda^2}{(\lambda + \alpha)^2} \sum_{i=1}^n y_i e^{-\lambda y_i}, \\
\frac{\partial^2 \ell_n(\phi)}{\partial \lambda \partial \theta} &= -\frac{\lambda}{\lambda + \alpha} \sum_{i=1}^n \left( \frac{\lambda + 2\alpha}{\lambda + \alpha} + \alpha y_i \right) y_i e^{-\lambda y_i}.
\end{aligned}$$

For large  $n$ , the expected information matrix  $\mathbf{I}_n(\phi) = E[\mathbf{J}_n(\phi)]$  is approximated by the negative hessian matrix:

$$\mathbf{J}_n(\phi) = - \begin{bmatrix} \frac{\partial^2 \ell_n(\phi)}{\partial \alpha^2} & \frac{\partial^2 \ell_n(\phi)}{\partial \alpha \partial \lambda} & \frac{\partial^2 \ell_n(\phi)}{\partial \alpha \partial \theta} \\ \frac{\partial^2 \ell_n(\phi)}{\partial \alpha \partial \lambda} & \frac{\partial^2 \ell_n(\phi)}{\partial \lambda^2} & \frac{\partial^2 \ell_n(\phi)}{\partial \lambda \partial \theta} \\ \frac{\partial^2 \ell_n(\phi)}{\partial \alpha \partial \theta} & \frac{\partial^2 \ell_n(\phi)}{\partial \lambda \partial \theta} & \frac{\partial^2 \ell_n(\phi)}{\partial \theta^2} \end{bmatrix}.$$

Under mild regularity conditions (see [17]), the asymptotic distribution of the MLE  $\hat{\phi}$  is multivariate normal distribution with mean  $\phi$  and variance-covariance matrix  $\mathbf{J}_n(\phi)$ .

#### 4. Simulation study

In this section, we conducted a simulation study to evaluate the performance of MLEs of the parameters  $\alpha, \lambda, \theta$  of GLP distribution. First, the following algorithm is used to generate a random sample  $Y_1, \dots, Y_n$ , from GLP distribution:

- (i) Generate  $U_i \sim U(0, 1)$ ,  $i = 1, \dots, n$ ;
- (ii) For  $i = 1, \dots, n$ , set

$$Y_i = \frac{1}{\alpha\lambda} \left[ -\alpha - \lambda - \alpha W_{-1} \left( -\frac{1 + \lambda/\alpha}{e^{1+\lambda/\alpha}} \cdot \frac{\log(e^\theta(1 - U_i) + U_i)}{\theta} \right) \right],$$

where  $W_{-1}$  denotes the negative branch of Lambert function.

The simulation experiment was repeated  $N = 3,000$  times each with sample size  $n = 25, 50, 75, 100, 200, 250$  and true parameters  $(\alpha, \lambda, \theta) = (0.5, 0.5, 0.5), (0.5, 0.5, 1), (1, 0.5, 1)$ . Four quantities were examined in this Monte Carlo study:

- (i) Bias of the MLE  $\hat{\nu}$  of the parameter  $\nu = \alpha, \lambda, \theta$ :

$$\text{Bias}(\hat{\nu}) = \frac{1}{N} \sum_{i=1}^N (\hat{\nu}_i - \nu);$$

- (ii) Mean-square error of the MLE  $\hat{\nu}$  of the parameter  $\nu = \alpha, \lambda, \theta$ :

$$\text{MSE}(\hat{\nu}) = \frac{1}{N} \sum_{i=1}^N (\hat{\nu}_i - \nu)^2;$$

- (iii) Coverage probability (CP) of 95% asymptotic confidence interval of the parameter  $\nu = \alpha, \lambda, \theta$ , i.e., the percentage of intervals containing the true value of  $\nu$ ;
- (iv) Average width (AW) of 95% confidence intervals of the parameter  $\nu = \alpha, \lambda, \theta$ .

Table 2 presents the biases and MSEs of the estimates which are seen to be small. This table also shows that the biases can be negative or positive and the MSEs decrease as the sample size increases.

Table 3 presents the coverage probabilities and average width of 95% confidence intervals of the parameters. This table shows that the coverage probabilities of the confidence intervals are quite close to the nominal level of 95% and that the average confidence widths decrease as the sample size increases, as one would expect.

TABLE 2. Bias and MSE of MLEs of  $\alpha$ ,  $\lambda$  and  $\theta$ .

$\alpha$	$\lambda$	$\theta$	$n$	Bias( $\hat{\alpha}$ )	Bias( $\hat{\lambda}$ )	Bias( $\hat{\theta}$ )	MSE( $\hat{\alpha}$ )	MSE( $\hat{\lambda}$ )	MSE( $\hat{\theta}$ )
0.5	0.5	0.5	50	0.2499	-0.0143	0.1449	0.5179	0.0188	0.6661
			100	0.1904	-0.0210	0.1157	0.3659	0.0124	0.5817
			150	0.1573	-0.0241	0.1345	0.2941	0.0097	0.5629
			200	0.1242	-0.0212	0.1135	0.2317	0.0081	0.5395
			250	0.1020	-0.0216	0.0920	0.1931	0.0069	0.4861
0.5	0.5	1.0	50	0.1317	0.0033	-0.1826	0.4407	0.0235	0.7289
			100	0.0765	-0.0100	-0.1822	0.3097	0.0152	0.6690
			150	0.0385	-0.0153	-0.1632	0.2276	0.0121	0.6598
			200	0.0039	-0.0156	-0.1906	0.1847	0.0104	0.6158
			250	-0.0133	-0.0198	-0.1648	0.1644	0.0090	0.6141
1.0	0.5	1.0	50	-0.0582	0.0050	-0.2622	0.5442	0.0205	0.8016
			100	-0.0243	-0.0058	-0.2373	0.4539	0.0145	0.7684
			150	-0.0016	-0.0098	-0.1625	0.4038	0.0111	0.6937
			200	-0.0202	-0.0099	-0.1799	0.3580	0.0100	0.6431
			250	-0.0137	-0.0090	-0.1382	0.3104	0.0088	0.6147

TABLE 3. Coverage probability and average width of the 95% CIs of  $\alpha$ ,  $\lambda$  and  $\theta$ .

$\alpha$	$\lambda$	$\theta$	$n$	CP( $\alpha$ )	CP( $\lambda$ )	CP( $\theta$ )	AW( $\alpha$ )	AW( $\lambda$ )	AW( $\theta$ )
0.5	0.5	0.5	50	0.9426	0.9673	0.9693	4.5945	0.7532	4.8948
			100	0.9800	0.9336	0.9300	3.7431	0.4538	3.2451
			150	0.9630	0.9270	0.9426	2.0231	0.3519	2.9816
			200	0.9566	0.9176	0.9346	1.6829	0.2985	2.4222
			250	0.9656	0.9240	0.9443	1.5734	0.2639	2.3136
0.5	0.5	1.0	50	0.9680	0.9346	0.9683	5.3984	0.6419	4.6306
			100	0.9640	0.9400	0.9536	2.2169	0.5201	4.5320
			150	0.9620	0.9530	0.9533	1.7792	0.5028	3.9401
			200	0.9376	0.9540	0.9450	1.1515	0.4613	3.7771
			250	0.9043	0.9086	0.9436	0.9094	0.2999	3.3715
1.0	0.5	1.0	50	0.9193	0.9613	0.9436	6.0639	0.6374	4.0840
			100	0.9633	0.9573	0.9400	4.5565	0.5441	3.8964
			150	0.9540	0.9453	0.9223	2.8769	0.4685	3.1382
			200	0.9526	0.9516	0.9260	2.3358	0.4672	3.0899
			250	0.9590	0.9303	0.9400	2.1272	0.3471	3.0551

## 5. Applications

In this section, we present the application of the GLP model to two real data sets to illustrate its flexibility among a set of competitive models with the following densities:

- (i) Lindley distribution ([9]).

$$f(y; \lambda) = \frac{\lambda^2}{1 + \lambda} (1 + y) e^{-\lambda y}, \quad y > 0, \quad \lambda > 0.$$

- (ii) Lindley-Poisson distribution ([10]).

$$f(y; \lambda, \theta) = \frac{\theta \lambda^2 (1 + y) e^{-\lambda y}}{(e^\theta - 1)(\lambda + 1)} e^{\theta \left(1 + \frac{\lambda y}{1 + \lambda}\right) e^{-\lambda y}}, \quad y > 0, \quad \theta, \lambda > 0.$$

- (iii) Weibull distribution

$$f(y; \alpha, \beta) = \frac{\alpha}{\beta} \left(\frac{y}{\beta}\right)^{\alpha-1} e^{-(y/\beta)^\alpha}, \quad y > 0, \quad \alpha, \beta > 0.$$

- (iv) Gamma distribution

$$f(y; \alpha, \beta) = \frac{1}{\Gamma(\alpha) \beta^\alpha} y^{\alpha-1} e^{-y/\beta}, \quad y > 0, \quad \alpha, \theta > 0,$$

where  $\Gamma(\cdot)$  is the gamma function.

To compare the GLP model with the above competing models, we use the following measures:

- (i) Log-likelihood function ( $\log(L)$ );
- (ii) Cramér-von Mises (CvM), Anderson-Darling (AD), and Kolmogorov-Smirnov (KS) test statistics;
- (iii)  $p$ -value of the KS test.

For a given data set, the selection criterion for the most suitable model is the one with largest  $\log(L)$ , smallest test statistic and largest  $p$ -value of the K-S test.

**5.1. Data set 1: The life of fatigue fracture data.** Here, we consider a data set representing the life of fatigue fracture of Kevlar 373/epoxy that are subject to constant pressure at the 90% stress level until all had failed (see [4]):

0.0251, 0.0886, 0.0891, 0.2501, 0.3113, 0.3451, 0.4763, 0.5650, 0.5671, 0.6566, 0.6748, 0.6751, 0.6753, 0.7696, 0.8375, 0.8391, 0.8425, 0.8645, 0.8851, 0.9113, 0.9120, 0.9836, 1.0483, 1.0596, 1.0773, 1.1733, 1.2570, 1.2766, 1.2985, 1.3211, 1.3503, 1.3551, 1.4595, 1.4880, 1.5728, 1.5733, 1.7083, 1.7263, 1.7460, 1.7630, 1.7746, 1.8275, 1.8375, 1.8503, 1.8808, 1.8878, 1.8881, 1.9316, 1.9558, 2.0048, 2.0408, 2.0903, 2.1093, 2.1330, 2.2100, 2.2460, 2.2878, 2.3203, 2.3470, 2.3513, 2.4951, 2.5260, 2.9911, 3.0256, 3.2678, 3.4045, 3.4846, 3.7433, 3.7455, 3.9143, 4.8073, 5.4005, 5.4435, 5.5295, 6.5541, 9.0960.

The total time on test (TTT) plot ([1]) for this data set is presented in Figure 3. This plot indicates that the hazard rate function is increasing.

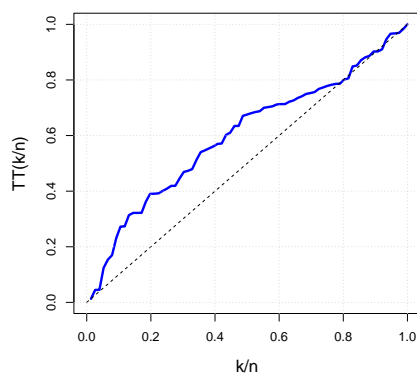


FIGURE 3. TTT plot for data set 1.

For all competing models, Table 4 shows the MLEs,  $\log(L)$ , CvM, AD, and KS statistics and  $p$ -value of the K-S test for data set 1. According to the selection criterion above, it is clear that GLP model is the most suitable for first data set. This conclusion is also supported by the graphical displays in Figure 4.

TABLE 4. Parameter estimates, log-likelihood values and goodness-of-fit measures for data set 1.

Model	MLE	$\log(L)$	CvM	AD	KS	$p$ -value
GLP	$\hat{\alpha} = 5.6784$ $\hat{\lambda} = 0.3447$ $\hat{\theta} = 5.6614$	-120.79	0.071	0.420	0.081	0.657
LP	$\hat{\lambda} = 0.7948$ $\hat{\theta} = 9.4 \times 10^{-8}$	-122.13	0.265	1.475	0.115	0.242
Lindley	$\hat{\lambda} = 0.7947$	-123.67	0.265	1.475	0.115	0.242
Weibull	$\hat{\alpha} = 1.3256$ $\hat{\beta} = 2.1326$	-122.52	0.135	0.788	0.109	0.295
Gamma	$\hat{\alpha} = 1.6412$ $\hat{\beta} = 1.1939$	-122.24	0.112	0.673	0.098	0.431

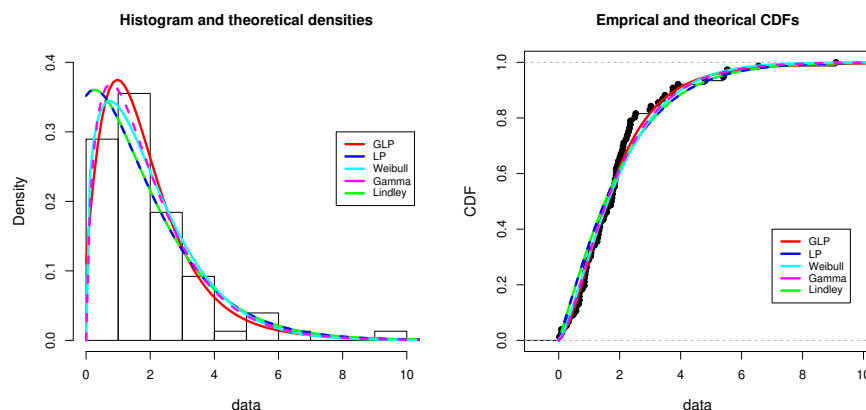


FIGURE 4. Diagnostic plots for fitted models for data set 1.

**5.2. Data set 2: UK COVID-19 data.** The second data represents a COVID-19 data belong to The United Kingdom of 76 days, from 15 April to 30 June 2020. These data formed of drought mortality rate. The data are as follows:

0.0587, 0.0863, 0.1165, 0.1247, 0.1277, 0.1303, 0.1652, 0.2079, 0.2395, 0.2751, 0.2845, 0.2992, 0.3188, 0.3317, 0.3446, 0.3553, 0.3622, 0.3926, 0.3926, 0.4110, 0.4633, 0.4690, 0.4954, 0.5139, 0.5696, 0.5837, 0.6197, 0.6365, 0.7096, 0.7193, 0.7444, 0.8590, 1.0438, 1.0602, 1.1305, 1.1468, 1.1533, 1.2260, 1.2707, 1.3423, 1.4149, 1.5709, 1.6017, 1.6083, 1.6324, 1.6998, 1.8164, 1.8392, 1.8721, 1.9844, 2.1360, 2.3987, 2.4153, 2.5225, 2.7087, 2.7946, 3.3609, 3.3715, 3.7840, 3.9042, 4.1969, 4.3451, 4.4627, 4.6477, 5.3664, 5.4500, 5.7522, 6.4241, 7.0657, 7.4456, 8.2307, 9.6315, 10.1870, 11.1429, 11.2019, 11.4584.

The data set is available at <https://covid19.who.int/>.

The TTT plot for this data set is presented in Figure 5. This plot indicates that the hazard rate function is decreasing.

For all competing models, Table 5 shows summary fit for data set 2. According to the selection criterion above, it is clear that GLP model is the most suitable for second data set. This conclusion is also supported by the graphical displays in Figure 6.

## 6. Conclusion and comments

In this paper, we have considered a generalized Lindley-Poisson distribution to analyze reliability/survival data where only the minimum of the sample

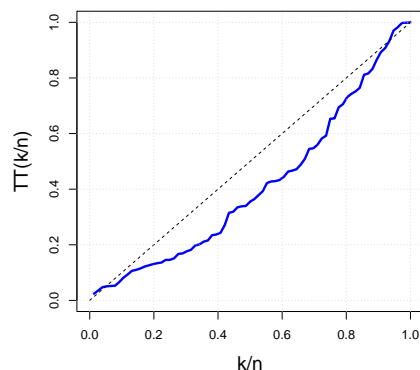


FIGURE 5. TTT plot for data set 2.

TABLE 5. Parameter estimates, log-likelihood values and goodness-of-fit measures for data set 2.

Model	MLE	$\log(L)$	CvM	AD	KS	$p$ -value
GLP	$\hat{\alpha} = 0.0006$ $\hat{\lambda} = 0.2546$ $\hat{\theta} = 1.8842$	-140.87	0.089	0.623	0.081	0.699
LP	$\hat{\lambda} = 2.2730$ $\hat{\theta} = 0.4530$	-145.16	0.358	2.473	0.140	0.099
Lindley	$\hat{\lambda} = 0.6578$	-150.94	0.938	5.847	0.201	0.004
Weibull	$\hat{\alpha} = 0.8464$ $\hat{\beta} = 2.2196$	-141.75	0.100	0.696	0.080	0.677
Gamma	$\hat{\alpha} = 0.8038$ $\hat{\beta} = 3.0323$	-142.41	0.160	0.974	0.096	0.455

from generalized Lindley distribution is observed and the sample size is a random variable having zero-truncated Poisson distribution. The resulting model is very flexible with decreasing, increasing, bathtub and increasing-decreasing-increasing shaped hazard rate function. The proposed model can be a viable alternative to well known models available in the literature and can be useful to analyze real data from wide range of applications.

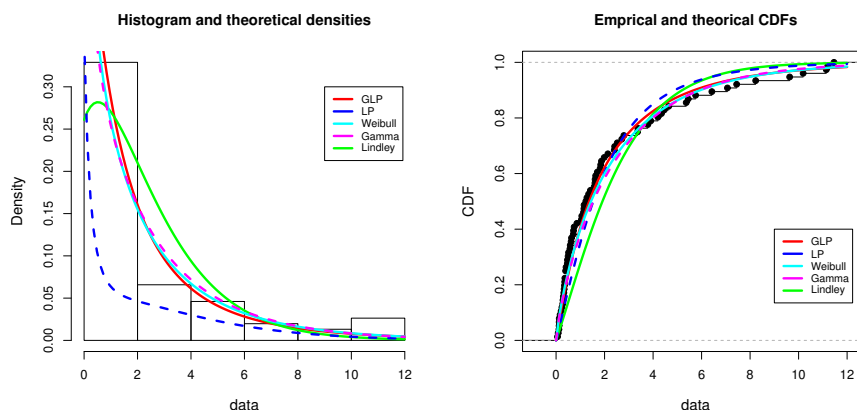


FIGURE 6. Diagnostic plots for fitted models for data set 2.

### References

- [1] M.V. Aarset, How to identify a bathtub hazard rate. *IEEE Transactions on Reliability*, **R-36** (1987), 106-108; DOI: 10.1109/tr.1987.5222310.
- [2] K. Adamidis, S. Loukas, A lifetime distribution with decreasing failure rate. *Statistics and Probability Letters*, **39** (1998), 35-42. DOI: 10.1016/s0167-7152(98)00012-1.
- [3] F. Almathkour, M. E. Ghitany, R. C. Gupta, J. Mazucheli, Analysis of survival data by a Weibull-generalized Sibuya distribution. *Austrian Journal of Statistics*, **51** (2022), 479-487; DOI:10.17713/ajs.v51i3.1273.
- [4] D. Andrews, A. Herzberg, Prognostic variables for survival in a randomized comparison of treatments for prostatic cancer. In: *Data: A Collection of Problems from Many Fields for the Student and Research Worker*, Springer, New York (1985).
- [5] W. Barreto-Souza, H.S. Bakouch, A new lifetime model with decreasing failure rate. *Statistics*, **47** (2013), 465-476; DOI: 10.1080/02331888.2011.595489.
- [6] M. Chahkandi, M. Ganjali, On some lifetime distributions with decreasing failure rate. *Computational Statistics and Data Analysis*, **53** (2009), 4433-4440; DOI: 10.1016/j.csda.2009.06.016.
- [7] F. Chapeau-Blondeau, A. Monir, Numerical evaluation of the Lambert W function and application to generation of generalized Gaussian noise with exponent  $1/2$ . *IEEE Transactions on Signal Processing*, **50** (2002), 2160-2165; DOI: 10.1109/tsp.2002.801912.
- [8] G.M. Cordeiro, J. Rodrigues, M. de Castro, The exponential COM-Poisson distribution. *Statistical Papers*, **53**, (2012), 653-664; DOI: 10.1007/s00362-011-0370-9.



- [9] M.E. Ghitany, B. Atieh, S. Nadarajah, Lindley distribution and its application. *Mathematics and Computers in Simulation*, **78** (2008), 493-506; DOI: 10.1016/j.matcom.2007.06.007.
- [10] W. Gui, S. Zhangy, X. Luz, The Lindley-Poisson distribution in lifetime analysis and its properties. *Haceteppe Journal of Mathematics and Statistics*, **36** (2014), 1063-1077.
- [11] R.C. Gupta, R.D. Gupta, General frailty model and stochastic orderings. *Journal of Statistical Planning and Inference*, **139** (2009), 3277-3287; DOI: 10.1016/j.jspi.2009.03.003.
- [12] R.C. Gupta, J. Huang, Analysis of survival data by a Weibull-generalized Poisson distribution. *Journal of Applied Statistics*, **41** (2014), 1548-1564; DOI: 10.1080/02664763.2014.881785.
- [13] R.C. Gupta, J. Huang, The Weibull Conway-Maxwell-Poisson distribution to analyze survival data. *Journal of Computational and Applied Mathematics*, **311** (2017), 171-182; DOI: 10.1016/j.cam.2016.06.035.
- [14] R. C. Gupta, M. Waleed, Analysis of survival data by a Weibull-Bessel distribution. *Communications in Statistics - Theory and Methods*, **47**, No 4 (2018), 980-995; DOI: 10.1080/03610926.2017.1316402.
- [15] P. Jodra, Computer generation of random variables with Lindley or Poisson-Lindley distribution via the Lambert W function. *Mathematics and Computers in Simulation*, **81** (2010), 851-859; DOI: 10.1016/j.matcom.2010.09.006.
- [16] C. Kus, A new lifetime distribution. *Computational Statistics and Data Analysis*, **51** (2007), 4497-4509; DOI: 10.1016/j.csda.2006.07.017.
- [17] L.E. Lehmann, G. Casella, Theory of point estimation (2nd ed.), Springer, New York (1998).
- [18] A.L. Morais, W. Barreto-Souza, A compound class of Weibull and power series distributions. *Computational Statistics and Data Analysis*, **55** (2011), 1410-1425; DOI: 10.1016/j.csda.2010.09.030.
- [19] M Pararai, G. Warahena-Liyanage, B.O. Oluyede, Exponentiated power Lindley Poisson distribution: Properties and applications. *Communications in Statistics - Theory and Methods*, **46** (2017), 4726-4755; DOI: 10.1080/03610926.2015.1076473.
- [20] R. Tahmasbi, S. Rezaei, A two-parameter lifetime distribution with decreasing failure rate. *Computational Statistics and Data Analysis*, **52** (2008), 3889-3901; DOI: 10.1016/j.csda.2007.12.002.
- [21] G. Warahena-Liyanage, M. Pararai, The Lindley power series class of distributions: Model, properties and applications. *Journal of Computations and Modelling*, **5** (2015), 35-80.